Applied Catalysis B: Environmental 88 (2009) 263–271

Contents lists available at ScienceDirect

Applied Catalysis B: Environmental

journal homepage: www.elsevier.com/locate/apcatb

Application of NO_X storage/release materials based on alkali-earth oxides supported on Al_2O_3 for high-temperature diesel soot oxidation

A.L. Kustov, M. Makkee *

Delft University of Technology, DelftChemTech, Catalysis Engineering, NL 2628 BL Delft, The Netherlands

ARTICLE INFO

Article history:
Received 31 August 2008
Received in revised form 4 November 2008
Accepted 9 November 2008
Available online 18 November 2008

Keywords:
Soot oxidation
Diesel particulate filter
NO_X storage/release
Alkali-earth catalysts

ABSTRACT

Alkali-earth oxides and nitrates supported on alumina were studied as model systems for NO_X storage/release. Their impact on the high-temperature soot oxidation has been investigated. The stability of surface nitrates and temperature of NO_X release increase parallel to the basicity of the cation. The presence of soot decreases the temperature of NO_X release. The storage capacity depends on the several factors, such as basicity, dispersion of the cation, and pre-treating conditions. Adsorption of NO with O_2 at 200 °C leads to the formation of surface nitrates that mainly exist as ionic nitrates. Stored nitrates contribute to the soot oxidation and assist to lower the temperature of soot oxidation up to almost 100 °C. In the presence of only NO_X storage material the efficiency of NO_X utilization is, however, quite low, around 30%. Therefore, the presence of an oxidation catalyst is essential to increase the efficiency of NO_X utilization for soot oxidation up to 140% and selectivity towards CO_2. A combination of oxidation catalyst with NO_X storage materials enables to lower the temperature of soot oxidation more than 100 °C for the Sr- and Ca-based systems.

© 2008 Elsevier B.V. All rights reserved.

1. Introduction

Soot or particulate matter (PM) and NO_X are the main pollutants in diesel engine emissions and represent health and environmental problems. Soot consists of carbon-based particles that are formed in a fuel-rich reaction zones, normally, around individual fuel droplets, where fuel hydrocarbons are oxidized under substoichiometric oxygen conditions, mainly by pyrolysis. In Euro 5 and 6 emission standards for cars and light trucks, which are expected to be implemented in 2009 and 2014, respectively, level of soot in exhaust should be decreased almost five times in comparison with Euro 4 regulations [1]. These standards cannot be achieved only by modifications of engine design or optimization of the fuel pre-treatment and combustion; therefore, an alternative way of treating diesel exhaust has to be developed [2]. Normally soot can be oxidized by oxygen to $CO + CO_2$ around 600 °C [3,4]. However, during most of the diesel engine operations the exhaust gas temperature is below 300 °C, which is too low to initiate continuous un-catalyzed soot oxidation. Soot is, therefore, collected on a filter and further can be oxidized at high temperatures to regenerate the filter. Several types of filters have been described in literature, but wall-flow monolith is by far the most studied and applied particulate trap. It consists of ceramic structure with parallel channels of which half are closed in an alternate checker board manner from upstream side and other half are closed at the downstream end. Thus, the exhaust gases are forced to flow through the porous walls that act as filters, in this way high particulate trapping efficiency can be achieved. However, in order to prevent clogging of the filter, it has to be regenerated from time to time.

In the easiest case of non-catalytic regeneration temperature is increased to initiate fuel combustion by air that is present in the exhaust. In this case temperatures above 600 °C are needed. However, supplying heat costs fuel and uncontrolled soot combustion can lead to high temperature gradients and, therefore, can damage the filter. As an alternative the use of catalysts in soot removal from particulate traps seems to be a logical choice, since catalysts for oxidation of carbonaceous materials have been studied for a long time. The one of the largest challenges arising here is solid–solid contact between catalyst and soot [3], since the activity of soot oxidation varies quite significantly depending on the contact. It was shown that in realistic conditions loose contact prevails and interaction between catalyst and soot is very limited, therefore, catalyst efficiency is low [5]. There are several approaches to overcome this problem, which will be addressed further.

Catalytically active material can be blended with fuel, in that case during fuel combustion active component is incorporated into the soot particle which ensures good contact between soot and catalyst. Fuel additives decrease the amount of soot formed due to

* Corresponding author. Tel.: +31 15 278 1391; fax: +31 15 278 5006.
E-mail address: m.makkee@tudelft.nl (M. Makkee).

0926-3373/$ – see front matter © 2008 Elsevier B.V. All rights reserved.
doi:10.1016/j.apcatb.2008.11.013

removal of soot precursors on early stage of soot formation and also soot oxidation at later stages. The most commonly used fuel additives are based on Ce, Pt, Cu, Fe, and Mn [6–8]. However, fuel additives cannot guarantee complete soot removal; therefore, frequent filter regenerations at higher temperatures should be also integrated.

It is also possible to improve the contact between soot and catalyst by applying systems with high catalyst mobility. This is normally a catalyst with a low melting point or high vapor pressure. This type of catalyst can be divided into three groups: metal oxides with low melting temperatures, like Sb_2O_3, MoO_3, V_2O_5 or PbO [9]; alkali carbonates or hydroxides, that form active and mobile alkali oxides or peroxides upon decomposition [2,10]; chlorides of transition metals [11] and molten salts [12,13]. However, because of insufficient stability and progressive loss of catalytic material, so far the application of the catalytic systems with mobile active component has proven to be inefficient [14,15].

It is possible to bypass the problem of poor contact if the role of the catalyst is only to provide active gaseous species during regeneration conditions (rich period) and restore them back during normal lean period. There are two principle active gaseous species that can be used to combust collected soot. Oxygen is the most obvious, since it is present in large quantities (5–10%) in diesel exhausts. Oxygen storage/release materials such as CeO_2 [16,17], rare-earth modified CeO_2 [18], perovskites [19], and spinel type oxides [20] can provide active oxygen. This active oxygen is transferred to soot by spillover mechanism and can initiate soot combustion at temperatures significantly lower than in the case of un-catalyzed soot oxidation. The 'active oxygen' of the oxygen storage components is capable of oxidizing soot around 450 °C which is still too high for continuous regeneration [16].

Contrariwise, nitrogen dioxide (NO_2) is known to be a more powerful oxidant than oxygen; therefore, it can convert soot to CO and CO_2 at temperatures as low as 275–300 °C [21,22]. In catalyzed soot filter (CSF) and continuously regenerating trap (CRT) NO in exhaust gas is converted to NO_2 by the oxidation catalyst and this NO_2 is further used to oxidize soot deposited on the filter. Such systems are successfully applied in the diesel engine systems where exhaust gases contain excess NO_X and exhaust gas temperatures are above 250 °C for significant amount of engine operating time.

Another possible strategy is to use a combination of oxidation catalyst and a NO_X storage material which will store the NO_X at temperatures of diesel engine operation, i.e. below 300 °C, as nitrates and release it during the phase of high-temperature regeneration [23,24]. In this case an oxidation catalyst will oxidize NO into NO_2 and, subsequently, the NO_2 will convert soot into CO and CO_2 and back to NO that can participate in the next soot oxidation event. In future combustion engines will likely to have lower NO_X emissions [25]; therefore, the efficient utilization of decreasing concentrations of NO in exhaust gases will be required. Since NO conversion to NO_2 is thermodynamically unfavourable at temperatures above 400 °C, it also has to be recycled to NO_2 with a very high efficiency. Therefore, platinum is most commonly added as an oxidation catalyst [22,26,27], since it cannot only effectively oxidize NO to NO_2, but also ensure complete conversion of unburned hydrocarbons and CO to harmless CO_2 and water. The principle of NO_X assisted soot particulate trap regeneration is schematically illustrated in Fig. 1.

As NO_X storage materials, alkali, alkali-earth, and rare-earth oxides clearly have potential, since they can store NO_X in form of nitrates and nitrites at low temperatures and release it as NO, NO_2, and active oxygen upon heating. Traditionally, Ba and K are the most reported NO_X storage systems, since they were also originally applied in the gasoline three-way systems [24,26,28–37]. CeO_2, ZrO_2, and La_2O_3 were also recently reported to store certain

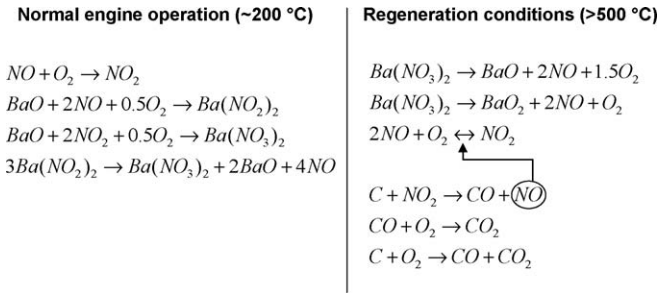

Fig. 1. Schematic representation of NO_X assisted soot oxidation.

amounts of NO_X, which can be later used for soot oxidation [38–40]. Several general observations about NO_X storage–release can be made from this literature:

- the amount of stored NO_X depends on the storage temperature, electro negativity and concentration of the storage component, and the nature of the support used;
- NO_X storage is accelerated in the presence of oxygen;
- nitrates are more stable than nitrites and represent dominant species at higher temperatures of NO_X adsorption;
- in many cases Pt decreases the stability of nitrates quite significantly.

For the practical application in diesel soot filter, storage/release system should store NO_X at temperatures around 200 °C and release it at higher temperatures between 400 and 500 °C, so that stored NO_X can be efficiently utilized for soot oxidation. At the same time stored nitrates should decompose before 600 °C, otherwise uncontrolled non-catalytic soot oxidation would take over. Among alkali-earth metals only Ba-based storage/release systems were applied for soot oxidation [24,26,30].

In this work for a first time we present a comparative and comprehensive study of the NO_X storage–release and subsequent soot oxidation on alkali-earth based catalytic systems. The influence of storage component on the NO_X storage capacity and the onset temperature of soot oxidation are analyzed. The estimates of the share and efficiency of NO_X utilization for the soot oxidation are presented.

2. Experimental

2.1. Materials

γ-Al_2O_3 (provided by Alfa Aesar, a Johnson Matthey Company, 99% purity) surface areas of 134 m^2/g was used as support materials. Model supported nitrates of Mg, Ca, and Sr (provided by Riedel-de Haën, 99% purity) were prepared by impregnation of a sieved fraction (0.065–0.35 mm) of the support with an aqueous solution of corresponding nitrates to obtain a final storage component concentration of 1000 μmol/g. For impregnation, the incipient wetness method was used, i.e. a defined volume of the solution was taken such that it was completely absorbed by the support material. With this technique, the content of introduced storage component can be controlled simply. Prior to impregnation, the supports were dried in an oven at 200 °C for 5 h. A period of about 4 h was allowed for the salt solution to homogeneously fill the pores of the support. In the case of Ba due to low solubility of barium nitrate, Ba was introduced using liquid adsorption: the amount of $Ba(NO_3)_2$ (provided by Riedel-de Haën, 99% purity) necessary to obtain final Ba concentration of 1000 μmol/g of the support was dissolved in the excess of water. Afterwards 5 g of powdered Al_2O_3 was added to that solution and resulting

suspension was stirred for 2 h; excess of water was further removed by evaporation. Subsequently, the impregnated supports were dried at room temperature for 12 h and heated in air up to 120 °C with a heating rate of 5 °C/min and kept at 120 °C for 2 h.

1 wt% Pt was introduced by incipient wetness impregnation using $Pt(NH_3)_4Cl_2{\cdot}H_2O$ (provided by Alfa Aesar, a Johnson Matthey Company, 56.4% purity) salt as precursor. Synthetic Printex-U soot from Degussa S.A., is used as a model soot whose characteristics are reported elsewhere [6].

2.2. Characterization

Surface area and porous properties of the samples were determined by N_2 physisorption at −196 °C in an automatic volumetric system (Autosorb-6, Quantachrome). BET-method was used to process the resulting adsorption isotherms.

The X-ray diffractogrammes are recorded in a Bruker D8 ADVANCE X-ray diffractometer with Ni-filtered Cu-Kα radiation (λ = 0.15418 nm). Data is collected between $2\theta = 20–80^\circ$ with a step size of 0.02.

The thermo gravimetric analysis (TGA) of the various samples was carried out in a Mettler Toledo, TGA/SDTA851e instrument. The samples (around 40 mg) were placed in alumina crucibles and loaded into TGA sample tray. All of the TGA data presented in this study were obtained by heating up the sample from 25 to 900 °C in air with a constant rate of 10 °C/min. Prior to sample analysis blank reference experiment with empty crucible was as a routine performed.

2.3. NO_X storage–release cycles and NO_X storage capacity

For storage–release of NO_X FT-IR Thermo Nicolet Nexus spectrometer using Spectratech diffuse reflectance accessory equipped with a high-temperature cell was used. OMNIC software was used to collect and process the spectra. Pfeiffer ThermoStar Mass spectrometer was coupled to the FT-IR unit. In standard experiment approximately 50 mg of sample was placed into the high-temperature ceramic cell. Further NO_X storage–release study was basically performed in three phases.

2.3.1. Decomposition of bulk nitrates in air

The temperature was increased from 200 to 600 °C with a 100 °C steps (heating rate of 30 °C/min) followed by an isotherm of 30 min at each temperature. Flow of 30 ml/min of He was used. With the increase of the temperature, bulk nitrate decomposes with the release of NO_X from the sample. The signal of evolving NO can be monitored by mass spectrometer (MS) and can be further used to calibrate MS signal, since the exact amount of nitrates in the starting sample is known (1000 μmol/g). It should be mentioned that mass spectrometric analysis of the decomposition products does not allow to distinguish between NO and NO_2 since both compounds have their main signal at m/e 30. Additionally due to fast reaction between NO and NO_2 in the presence of oxygen NO and NO_2 are always present in equilibrium concentrations; therefore, further the signal at m/e 30 will be referred to as NO_X, where $X = 1$ or 2. After the decomposition of bulk nitrates background spectra were collected from 600 to 200 °C with 100 °C steps.

2.3.2. Storage of NO_X

The sample obtained after the previous step was treated at 200 °C with a flow of 800 ppm of NO + 20% of O_2 in He (30 ml/min) and NO is adsorbed on the surface of the catalyst with the formation of nitrates and nitrites. At the same time FT-IR spectra were collected every 2–5 min until no changes were observed in the spectra.

2.3.3. Desorption of stored NO_X

The flow of NO was switched off and the temperature was increased from 200 °C until 600 °C with 100 °C step in He or 20% of O_2 in He mixture (30 ml/min). The decomposition of nitrates was monitored by FT-IR and the products were analyzed by MS. By the comparison of the amount of the released NO_X with the theoretically possible amount of nitrates (determined in Section 2.3.1) it is possible to estimate the amount of the storage component involved into the NO_X storage. The storage capacity is calculated using following formula:

$$\text{Storage capacity}\,(\%) = \frac{\text{amount of desorbed NO}_X\,(\text{mmol/g}_{\text{cat}})}{2 \times \text{amount of storage cation}\,(\text{mmol/g}_{\text{cat}})} \times 100$$

2.4. Soot oxidation

Soot oxidation is studied by temperature programmed reaction method. If not mentioned otherwise, prior to the measurements soot was mixed with catalyst and silicium carbide as dilutant in proportion of 1:20:120 with a spatula in order to obtain a loose contact mode. In the typical experiment approximately 200 mg of sample is packed between two quartz wool plugs and is carried out in a tubular quartz reactor (5 mm internal diameter). Reactor is heated from room temperature to 900 °C with a heating rate of 5 °C/min in a flow of 20% of O_2 in He (total flow 50 ml/min). Reaction products are analyzed by Balzer mass spectrometer. Using the areas under CO– and CO_2– signals and assuming complete soot combustion at the end of the experiment at 900 °C soot conversion at each temperature and selectivity of soot oxidation to CO_2 can be quantified:

$$\text{Conversion}\,(\%) = \frac{S_{CO}(T) + S_{CO_2}(T)}{S_{CO}^{tot} + S_{CO_2}^{tot}} \times 100$$

where $S_{CO}(T)$ and $S_{CO_2}(T)$ represent areas under the CO and CO_2 curves at selected temperature T and S_{CO}^{tot} and $S_{CO_2}^{tot}$ represent areas under the CO and CO_2 curve at 900 °C.

$$\text{Selectivity}\,(\%) = \frac{S_{CO_2}^{tot}}{S_{CO_2}^{tot} + S_{CO}^{tot}} \times 100$$

3. Results and discussion

3.1. Physicochemical properties

According to the N_2 adsorption–desorption measurements, all samples show a similar type IV isotherm with corresponding hysteresis. The pore size distributions of the various samples show a perfect overlay (~10 nm), apart from minor difference in intensity. Noticeably, after the impregnation BET surface area and total pore volume decreases slightly and the decrease is proportional to the size of cation introduced (Table 1).

According to the XRD phase analysis in the case of barium and strontium more bulky nitrate particles are formed, while in the case of calcium and magnesium, nitrates are more uniformly dispersed over the support. After calcination all the signals from bulk phases disappear indicating the reconstruction of nitrate species from bulky particles to XRD invisible thin oxide layers or particles smaller than 20 nm. It is possible to make a simple estimation, based on the crystal unit size of barium nitrate (8.11 Å) and barium oxide (5.54 Å) [41,42] and assuming layer coverage of Al_2O_3 support. In the case of $Ba(NO_3)_2$ almost three monolayers can be formed, while after calcination and transformation to BaO coverage slightly exceeding monolayer (1.3–1.4 monolayers) can be obtained. Ca and Mg oxides have significantly smaller lattice

Table 1
Physicochemical properties of the catalysts.

Sample	BET surface area (m^2/g)	Total pore volume (cm^3/g)	Phases detected
γ-Al_2O_3	135	0.43	Amorphous
$Ba(NO_3)_2/Al_2O_3$	105	0.35	Ba(NO3)2
$Sr(NO_3)_2/Al_2O_3$	112	0.37	Sr(NO3)2
$Ca(NO_3)_2/Al_2O_3$	117	0.39	Amorphous
$Mg(NO_3)_2/Al_2O_3$	122	0.40	Amorphous

parameters (4.81 and 4.20 Å, respectively); therefore, even better distribution of the storage component over the surface of Al_2O_3 should be expected.

3.2. Decomposition of bulk nitrates

For the practical application in soot trap storage compound should release nitrates at temperatures above 400 °C. Therefore, decomposition of model nitrates was initially analyzed by gravimetric analysis. The derivative of the weight loss versus temperature for alkali-earth nitrates is shown on Fig. 2. According to this data, in the case of magnesium, nitrates are decomposed too early, around 200 °C, so most of the nitrates will be released before the regeneration, just during normal engine conditions. In case of barium, nitrates are very stable and decompose only at around 600 °C, which seems rather unpractical, since un-catalyzed soot oxidation also starts in this region and there will be no benefit in the temperature of the soot oxidation. Of course, barium based system still should not be discarded, because the presence of the driving force (for example a reducing atmosphere) is known to facilitate the decomposition of nitrates [32,43]. Based on the temperatures of nitrates decomposition strontium and calcium-based systems look most promising: those nitrates are mainly decomposed around 400–500 °C. However, it should be pointed out that these results are obtained for mainly bulk nitrates and from practical point of view actual stored nitrates are of a considerable interest. Therefore, the next step is to study all these systems in the storage–release cycles.

3.3. NO_X storage–release

The storage–release of NO_X on different model systems was studied with the use of DRIFT cell coupled to the MS. The first step is the decomposition of bulk nitrates into corresponding oxides, which allows calibrating MS signal, since the amount of NO_X that should be released upon thermal decomposition is known. The decomposition profiles (not shown here for the sake of brevity) are very consistent with the TGA results with only difference: the temperature is increased stepwise (not continuously like in the case of TGA experiments).

During the storage stage NO is adsorbed by alkali-earth oxides from the mixture of 800 ppm of NO + 20% of O_2 in He at 200 °C, while FT-IR spectra are recorded. The evolution of the spectra with the increase of the adsorption time for pure Al_2O_3 and supported oxides are shown on Figs. 3–7.

It is possible to observe that already after few minutes some bands, characteristic to nitrate species appear in the region 1200–1800 cm^{-1}. Further these bands progress and some new bands in this region become visible until saturation with nitrates is reached and spectra do not change anymore. Noteworthy, according to the FT-IR results most of the NO_X is adsorbed within the first 20–30 min. After certain time the spectrum does not change, which

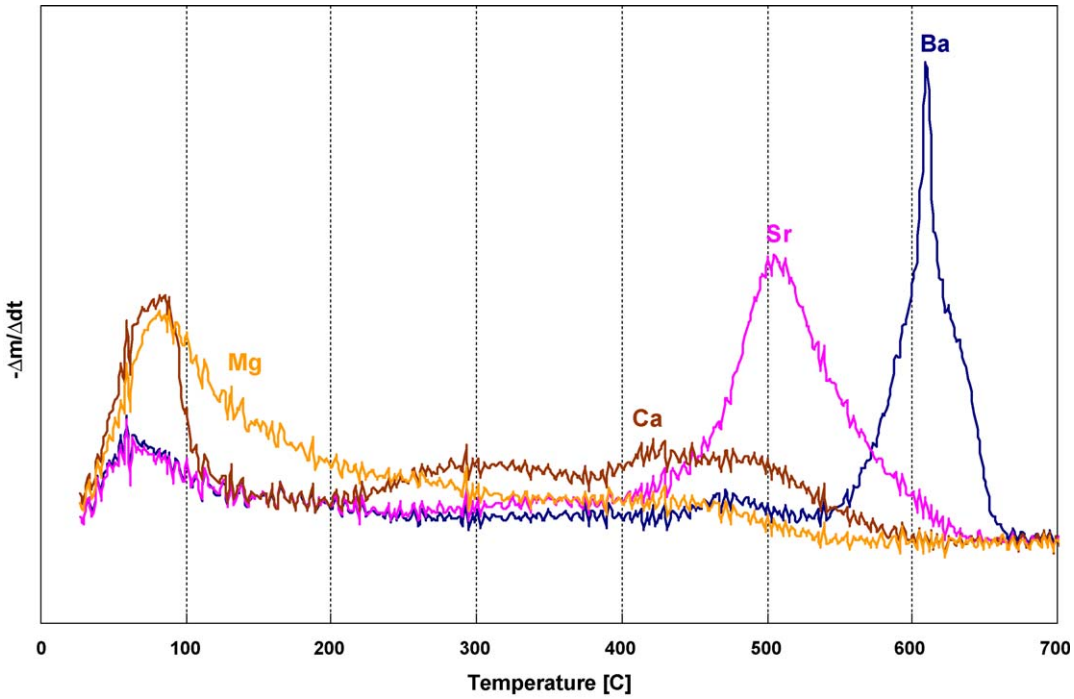

Fig. 2. Differential thermogravimetric profiles in air for decomposition of bulk nitrates of Mg, Ca, Sr, and Ba supported on Al_2O_3. Decomposition conditions: 100 ml/min air, 10 °C/min.

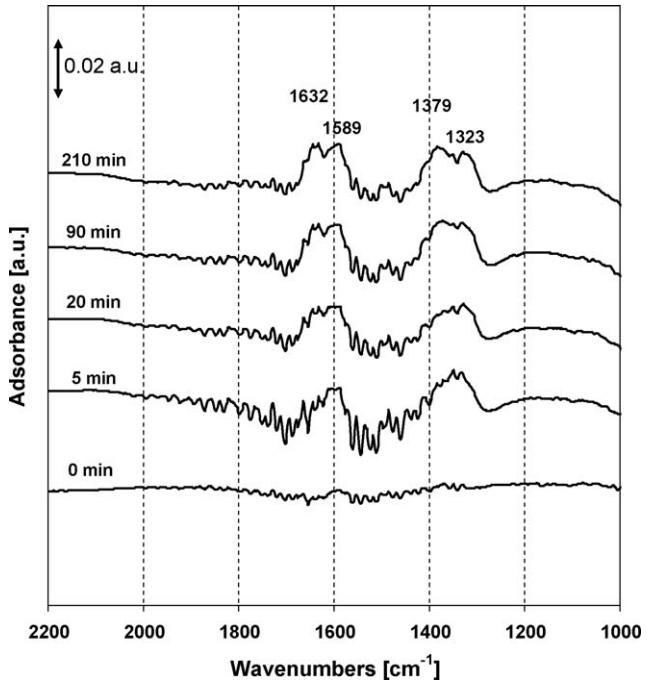

Fig. 3. FT-IR spectra upon adsorption of 800 ppm NO in 20% O_2 in He mixture on Al_2O_3 at 200 °C.

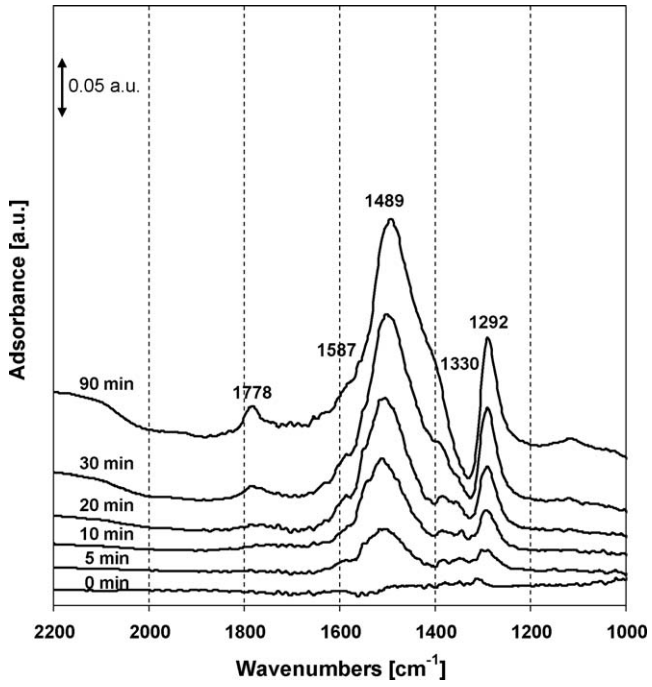

Fig. 5. FT-IR spectra upon adsorption of 800 ppm NO in 20% O_2 in He mixture on Sr/Al_2O_3 at 200 °C.

means that adsorption is finished. It takes about 1–2 h to reach complete saturation.

Upon admission of the NO/O_2 mixture on pure alumina (Fig. 3) weak bands at 1330 and 1590 cm^{-1} were formed. According to Refs. [37,44] these bands can be assigned to surface chelating bidentate nitrates. Chelating nitrates reached the maximum intensity after approximately 5 min of contact, while the formation of bridging bidentate nitrates at 1632 and 1379 cm^{-1} continued. The main surface species observed after 90 min of contact with the NO/O_2 mixture were bridging and chelating bidentate nitrates in agreement with results of Prinetto et al. [44].

For supported Ba, Sr, Ca, and Mg systems (Figs. 4–7) the band assignments is not straightforward due to the great number of NO_X species formed. On Ba/Al_2O_3 catalyst (Fig. 5), a variety of bands are formed in the 1800–1200 cm^{-1} region, all intensities increase with the contact time. These bands can be assigned to different types of NO_X surface species [37,42,43]. In the case of the Ba-containing catalysts, the main species formed upon NO/O_2 adsorption were

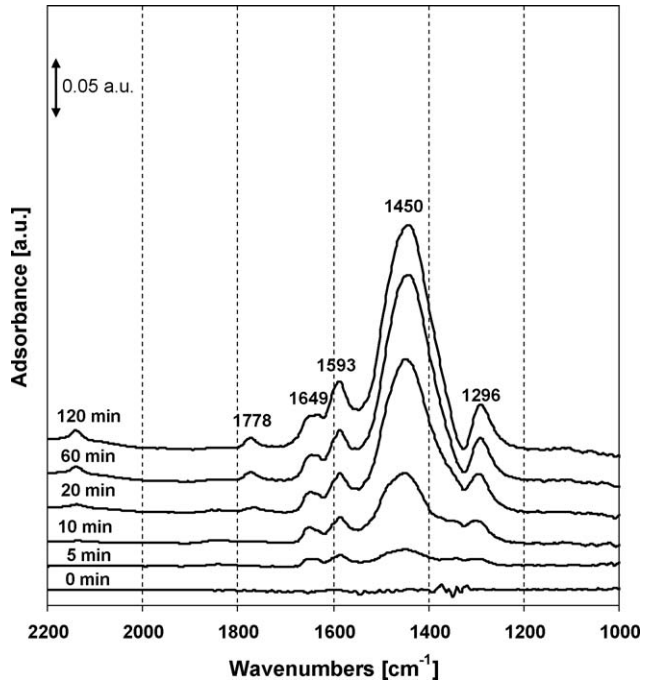

Fig. 4. FT-IR spectra upon adsorption of 800 ppm NO in 20% O_2 in He mixture on Ba/Al_2O_3 at 200 °C.

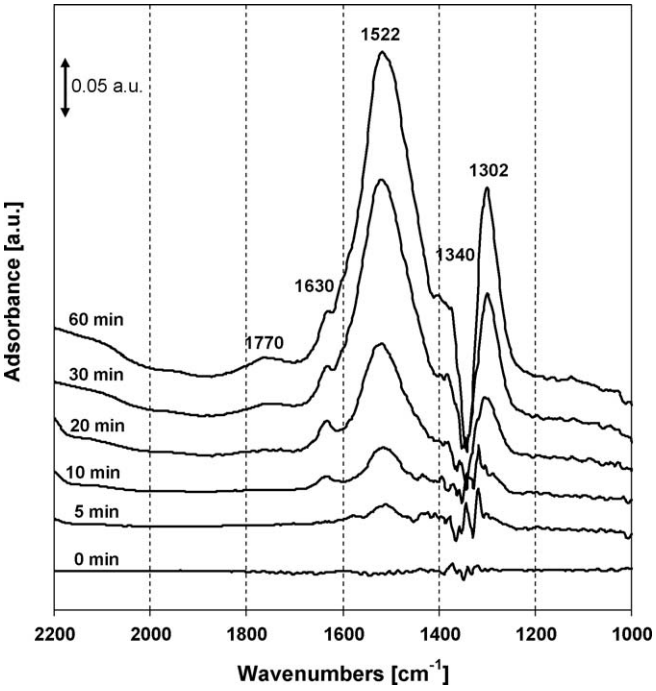

Fig. 6. FT-IR spectra upon adsorption of 800 ppm NO in 20% O_2 in He mixture on Ca/Al_2O_3 at 200 °C.

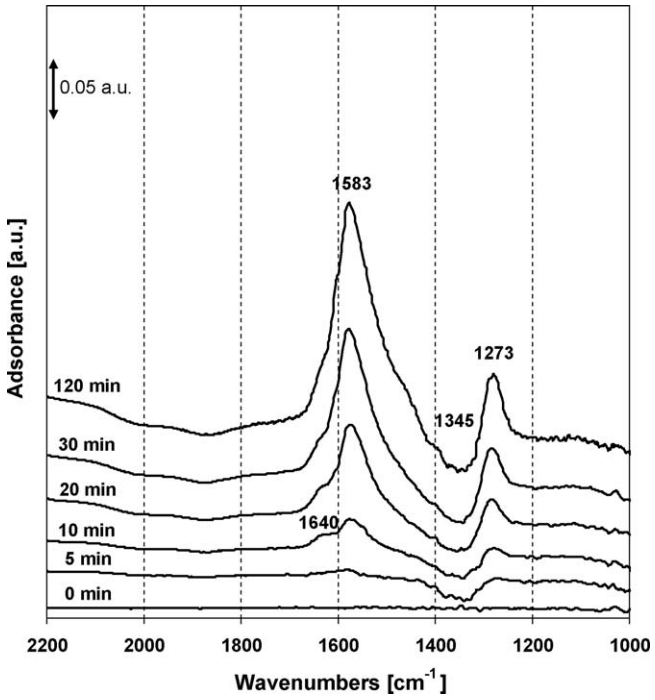

Fig. 7. FT-IR spectra upon adsorption of 800 ppm NO in 20% O_2 in He mixture on Mg/Al_2O_3 at 200 °C.

ionic (1450 and 1352 cm^{-1}) and bidentate (chelating and/or bridging at 1320–1210 and 1650–1540 cm^{-1}) nitrates, whereas nitrites and $NO_2^{\delta+}$ species were not detected. Weak band at 1778 cm^{-1} can be assigned to the formation of nitrosyl M–ON^- or M–NO^- species. The complexity of the absorptions and partial overlapping of the bands assigned to bidentate nitrates do not allow distinguishing between different types of nitrate species and could reflect the heterogeneity of surface sites. Similar sets of bands are observed for other alkali-earth containing catalysts. Noteworthy the major band assigned to ionic nitrate species gradually shifts form 1450 cm^{-1} in the case of Ba towards 1583 cm^{-1} for Mg, parallel with the decrease of the basicity of the cation, which reflects the shortening of the distance $M^{\delta+}$–$(NO_3)^{\delta-}$ in ionic nitrates in the change from Ba towards Mg.

In all adsorption spectra, except pure alumina negative band at ~1430 cm^{-1} can be clearly observed. According to the explanation suggested in [44] this negative band arose from the strong superposition of the vibrational modes of ionic nitrates with those of carbonates which decrease during the conversion of carbonates and/or oxides into nitrates upon interaction with a NO/O_2 mixture.

It should be noted that unlike several other works on adsorption of NO or NO/O_2 mixtures on different oxides [37,44,45] no clear bands, that can be reliably assigned to the formation of nitrite species, have been observed in this work. Possible explanation of this fact is that in this work adsorption studies were performed at 200 °C. It is described in literature [33,44] that at high temperatures nitrites can undergo transformation to nitrates, according to the following reaction, which is considered to be the main path of nitrites decomposition:

$$3Ba(NO_2)_2 \rightarrow Ba(NO_3)_2 + 2BaO + 4NO$$

For example, in the work of Prinetto et al. [44] nitrites were observed to be the prevailing species at room temperature on Ba/Al_2O_3 and $Pt–Ba/Al_2O_3$ systems but already at 200 °C most of the nitrites were decomposed with the formation to the corresponding nitrates.

During the third step, the flow of NO is switched off and desorption in air is performed with the increasing of the temperature from 200 until 600 °C. The decomposition of surface nitrates proceeds according to the reaction similar as in the case of bulk nitrates. Desorbed species are again detected by MS so it is possible to determine amounts of NO_X desorbed. The desorption results are summarized in Table 2. T_{bulk} and $T_{surface}$ are the temperature intervals corresponding to the maximums of decomposition of bulk and stored/surface nitrates. Storage capacity in % reflects the share of storage component involved in NO_X storage compared to 100% for the model bulk nitrates. The amount of NO_X desorbed from Al_2O_3 is very small (below few μmol/g) and, therefore, can be neglected.

Table 2
NO_X desorption characteristics and storage capacities of different samples determined using FT-IR-MS results.

System	T_{bulk} (°C)	$T_{surface}$ (°C)	NO_X desorbed (μmol/g)	Storage capacity (%)
$Ba(NO_3)_2/Al_2O_3$	610	>600	114	5.7
$Sr(NO_3)_2/Al_2O_3$	505	600	330	16.5
$Ca(NO_3)_2/Al_2O_3$	300–450	500–600	498	24.9
$Mg(NO_3)_2/Al_2O_3$	200–350	400	122	6.1

Several observations can be made based on the comparison of the systems (Table 2): (1) the storage capacity is far from being optimal, indicating that most of the storage component does not participate in nitrates storage and (2) the surface nitrates have somewhat higher stability than bulk nitrates, so except magnesium-based system the major part of nitrates is released at temperatures above 500 °C. Possible explanation of this phenomenon can be related to the heterogeneous nature of the surface nitrate species. Even during the decomposition of the model nitrates (Fig. 2) it was found that nitrates in most cases decompose in a rather broad temperature window. Therefore, from the thermodynamic point of view and taking into account the fact that only a fraction of storage component participates into NO_X adsorption followed by the formation of nitrates, it is reasonable to expect that upon interaction with NO_X initially most stable nitrates will be formed. Another option is that during the decomposition of the model nitrates at 600 °C bulky particles formed during the impregnation procedure are transformed into smaller oxide particles or thin layers (as was observed in XRD). In this way the stability of forming surface nitrates could be higher due to the possibility of nitrate species interaction with more than one atom of alkali-earth adsorption component.

The available storage capacity increases from barium to calcium, which can also be related with the difference in the availability of the storage component. For magnesium-based system storage is quite low probably due to the fact that most of the stored nitrates are decomposed at storage conditions (200 °C). It should be pointed out that due to technical restrictions cell used for NO_X storage–release studies could not be heated to more than 600 °C. Therefore, the storage capacities presented in Table 2 reflect the amount of stored NO_X which can be released up to 600 °C. There is high possibility that in the case of Ba or even to some extent of Sr some stored nitrates will still be present on the storage component at temperatures higher than 600 °C. From practical point of view these nitrates, due to their high thermal stability, have little use for filter regeneration, since their decomposition would require either too high temperatures or the presence of strong driving force in the exhaust (for example, the presence of reductant could help to lower the temperature of NO_X release quite significantly [32,43]). Ba-based storage systems have been studied quite intensively for their application in TWC [26,28–36]. The reported storage capacities and amount of desorbed NO_X differ, however, quite significantly because of the difference in catalyst composition/preparation and storage conditions. For example in the works of Gilot and co-workers [33,34]

Table 3
Influence of soot:catalyst ratio on overall soot oxidation. Reaction conditions: temperature from room temperature to 900 °C, heating rate of 5 °C/min in a flow of 10 ml/min of O_2 and 40 ml/min of He, loose contact.

Sample	N/C ratio	$Tmax_1$ (°C)	$Tmax_2$ (°C)	Share of NO_X assisted soot oxidation (%)	$T_{20\%}$ (°C)
Soot + Al_2O_3 (1:5)	–	–	633	–	584
Soot + $Sr(NO_3)_2/Al_2O_3$ (1:5)	0.13	507	635	5.2	539
Soot + $Sr(NO_3)_2/Al_2O_3$ (1:10)	0.25	503	620	6.0	519
Soot + $Sr(NO_3)_2/Al_2O_3$ (1:20)	0.50	502	610	9.1	509
Soot + $Sr(NO_3)_2/Al_2O_3$ (1:50)	1.28	515	565	40.6	489

for different model and commercial Ba-containing storage systems the amount of stored NO_X was ranging from 50 to 700 μmol/g depending on storage temperature, gas composition, and Ba content. Large difference between amounts of stored and released NO_X was reported by Medhekar et al.: 150 μmol/g versus 42 μmol/g for model 1.3% Pt-17% BaO/Al_2O_3 catalyst, respectively [46]. In several works [26,33,43] optimal temperature for NO_X storage for Ba/Al_2O_3 systems was found to be around 350–400 °C, which is significantly higher than that in the present study (200 °C). Nevertheless, in most cases reported storage capacities were far below possible 100%.

Therefore, the possibility to enhance storage capacity by means of different catalysts pre-treatment was studied in the case of Sr/Al_2O_3 system. Three different pre-treatment procedures were tested. In the first experiment sample was pre-treated in He at 600 °C resulting in the storage capacity of 17%. Pre-treating in air led to an increase of the amount of stored NO_X to 27% and the amount of NO_X desorbed between 200 and 500 °C also increased quite significantly. The most pronounced increase of the storage capacity was obtained after pre-treating in reducing atmosphere (5% H_2 in He at 500 °C), resulting in a storage capacity of more than 40%. The effect of the different pre-treating conditions may be related with the redispersion of the storage component and its better resulting availability for NO_X storage.

3.4. Soot oxidation

With the increase of the temperature nitrates start to decompose with the release of nitrogen dioxide that reacts with soot forming CO, CO_2 and back to nitrogen monoxide. The products of this reaction were continuously monitored by MS.

The typical results of TPD experiment for $Sr(NO_3)_2/Al_2O_3$ sample are shown on Fig. 8A, where signals of NO, CO, and CO_2 can be used to determine concentrations of these components in outlet of the reactor. The combination of CO and CO_2 signal allows us to calculate the soot conversion, by assuming that all soot is converted to CO and CO_2 at the end of the desorption experiment (900 °C). Similar curves were obtained for all other systems but not presented here for the sake of brevity. It is possible to make a deconvolution of CO_2 signal into two components as shown on Fig. 8B, so the first, low-temperature peak corresponds to the soot oxidation with NO_2 and its temperature coincide with the temperature of nitrates decomposition, while the second peak represents un-catalyzed soot oxidation with oxygen. For deconvolution log-normal peak fitting was used, where position of the maximum of the first peak was fixed to be the same as maximum temperature of NO_X signal. By making this deconvolution and comparing areas of two resulting peaks it is possible to estimate the contribution of NO_X to overall soot oxidation. It should be noted that such deconvolution of soot oxidation profile involves some spread of the results, related with close positioning and not perfect separation of both peaks. However, the main trends should be considered reliable, because similar deconvolution procedures were used in all cases.

There is a possibility that CO_2 produced during soot combustion can be first stored on the catalysts as carbonates, thus masking the NO_X assisted soot oxidation. However, carbonates have a much lower stability than nitrates; for example the standard Gibbs energy of the decomposition of $Ca(CO_3)$ is 129 kJ/mol, while the Gibbs energy of $Ca(NO_3)_2$ decomposition is almost twice higher, 240 kJ/mol. Stability of alkali-earth carbonates follows the similar trend as for nitrates, i.e. increases with the basicity of the cation according to thermodynamic reaction data [47]. This indicates that at the temperatures of nitrates decomposition (above 200 °C) the stability of corresponding carbonates will be very low (much lower than nitrates) and, therefore, effect of carbonate formation can be neglected at elevated temperatures applied in this study.

The influence of the catalyst:soot ratio was studied and results are summarized in Table 3. Here $Tmax_1$ and $Tmax_2$ correspond to the maximum temperatures of soot oxidation by NO_X and oxygen, respectively; the ratio between these two peaks gives the share of NO_X assisted soot oxidation, and $T_{20\%}$ is temperature of 20% soot conversion. The sample "soot + Al_2O_3 (1:5)" represent un-catalyzed soot oxidation. The temperature of soot oxidation in this case

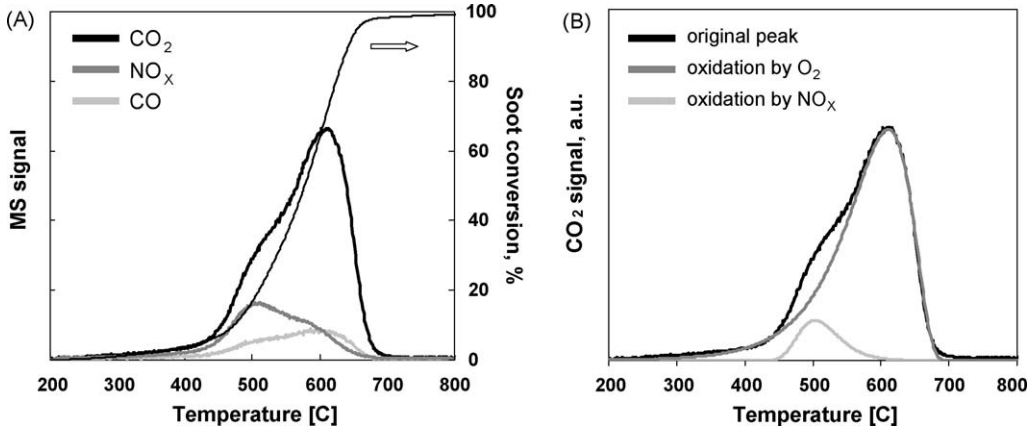

Fig. 8. TPD profiles of CO_2, CO, and NO_X signals and calculated soot conversion (A) and deconvoluted CO_2 signal (B) for $Sr(NO_3)_2/Al_2O_3$ sample. Reaction conditions: increase of temperature from room temperature to 900 °C, heating rate of 5 °C/min in a flow of 10 ml/min of O_2 and 40 ml/min of He. Soot:catalyst:SiC ratio of 1:20:120, loose contact.

is quite high, around 600 °C, which is far above desired regeneration temperature. After introduction of even small amounts of stored nitrates into the system the temperature of soot oxidation decreases quite significantly. With further increase of the concentration of nitrates temperature decreases even further up to 490 °C which is almost 100 °C lower than in the case of the un-catalyzed soot oxidation. It can be noticed that the temperature of nitrates decomposition $T\max_1$ is decreasing in the presence of soot, from 552 °C for $Sr(NO_3)_2/Al_2O_3$ system to 500 °C for soot + $Sr(NO_3)_2/Al_2O_3$ (1:20), which can be stipulated by the presence of driving force due to reaction between forming NO_X and soot.

If we compare the amount of available NO_X with the share of NO_X assisted soot oxidation it is possible to estimate the efficiency of NO_X utilization. Indifferent on the ratio between catalyst and soot this efficiency appears to be relatively low, around 20–30%. This can be related with decreased thermodynamic stability of nitrogen dioxide at higher temperatures: after decomposition of nitrates NO_2 is released, which, at temperatures above 400 °C, is converted to thermodynamically more stable nitrogen monoxide. Nitrogen monoxide is much weaker oxidant than NO_2. In order to improve the utilization of decreasing amount of NO_2 it should, therefore, be recycled back.

The results of soot oxidation for model nitrate-containing systems with different alkali-earth cations are presented in Fig. 9. The temperature of 20% soot conversion reflects the activity of given catalysts for soot oxidation. The share of soot oxidation by NO_2 among all soot oxidation reactions is determined by the deconvolution of CO_2 signal and gives an impression about the efficiency of the catalysts. After introduction of the storage component the temperature of soot oxidation decreases quite significantly in comparison with un-catalyzed soot oxidation and keeps decreasing in parallel to the decrease of the stability of nitrates. The lowest temperature is achieved for calcium around 485 °C. Magnesium falls out of general trend which can be explained by insufficient stability of nitrates in this system: magnesium nitrates are decomposed too early, around 200 °C, and this temperature is too low to initiate the reaction between soot and NO_2. The efficiency of NO_X utilization is rather low for all systems except for calcium-based catalyst. This indicates that most of the nitrogen oxides released does not participate in soot oxidation.

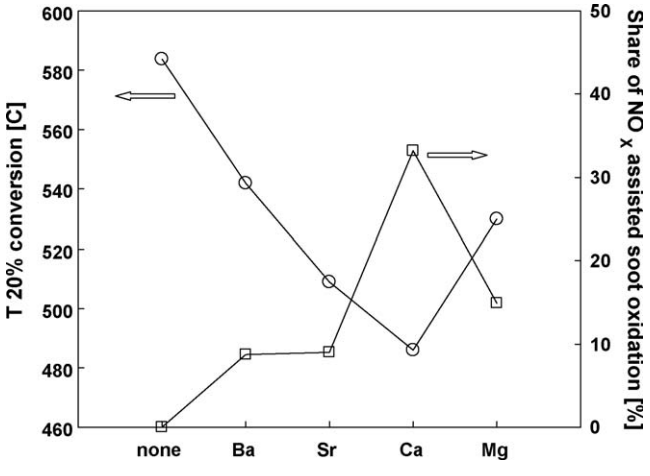

Fig. 9. Influence of alkali-earth cation M on $T_{20\%\ conversion}$ (○) and share of NO_X assisted soot oxidation (□) in the system soot + $M(NO_3)_2/Al_2O_3$. Reaction conditions: temperature from room temperature to 900 °C, heating rate of 5 °C/min in a flow of 10 ml/min of O_2 and 40 ml/min of He. Soot:catalyst:SiC ratio of 1:20:120 (N/C ratio = 0.25), loose contact.

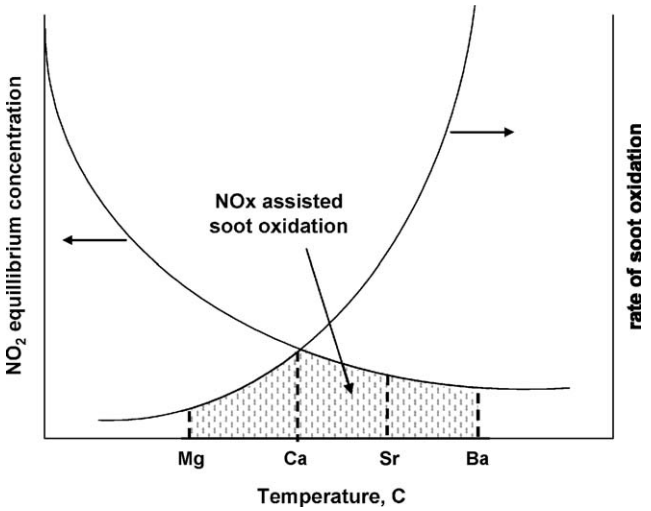

Fig. 10. Schematic explanation of NO_X assisted soot oxidation for different alkali-earth metals. The rate of NO_X assisted soot oxidation is limited from one side equilibrium concentration of NO_2 and from the other side, kinetics of soot oxidation. Optimal interval coincide with temperature of the decomposition of $Ca(NO_3)_2$.

Apparently, the most efficient soot oxidation is achieved in the case when there is a match between the temperature of the nitrates decomposition and temperature of soot oxidation by NO_2. The explanation of the observed trend for soot oxidation in the presence of nitrates of different alkali-earth metals can be schematically represented as illustrated on Fig. 10. The rate of NO_X assisted soot oxidation is limited from one side by equilibrium concentration of NO_2, which decreases significantly as the temperature increases. From the other side, at low temperatures the reaction is limited by the kinetics of the soot oxidation, since, accordingly to the experiments with soot oxidation by gaseous NO_2, sufficient reaction rates are observed only above 300 °C [21,22]. Therefore, optimal interval for NO_X release should be between 350 and 450 °C, which coincide with temperature of the decomposition of $Ca(NO_3)_2$. Therefore, the decrease in the temperature of 20% soot conversion is most pronounced for the Ca-based system as can be seen from Fig. 9.

It should be also taken into account that soot combustion is exothermic reaction. Therefore, some heat produced locally during the soot oxidation by NO_2 can be utilized either to initiate the soot oxidation by oxygen or can promote further the decomposition of nitrates, which is an endothermic process. In both ways the increased rate of soot oxidation will be observed and in this study all these contributions are considered as NO_X assisted soot oxidation, since it correlates with the temperature of nitrates decomposition and it is also impossible to distinguish between them. This effect can also partially account for the very high efficiency of calcium-based system in comparison with other storage components.

To improve the utilization of decreasing amount of NO_2 at elevated temperatures it should be recycled back every time after it participates in single soot oxidation step. It can be achieved by combining NO storage material with the oxidation catalyst, from which Pt is an obvious choice [22,26,27]. The comparative results of soot oxidation for nitrate-containing systems with and without Pt are summarized in Table 4. According to these results platinum itself has very little effect on the temperature of soot oxidation, even though, it increases the selectivity of soot conversion to CO_2. In the systems where Pt is present in the combination with NO_X storage component the temperature of soot oxidation is decreased quite substantially in comparison with the only nitrates-containing catalysts. The efficiency of NO oxidation to NO_2 on Pt/Al_2O_3

Table 4
Influence of oxidation function on overall soot oxidation. Reaction conditions: temperature from room temperature to 900 °C, heating rate of 5 °C/min in a flow of 10 ml/min of O_2 and 40 ml/min of He. Soot:catalyst:SiC ratio of 1:20:120 (N/C ratio = 0.25), loose contact.

Catalyst	$T_{20\%}$ (°C)	S_{CO_2} (%)	Efficiency of NO_X utilization (%)
Al_2O_3	584	88	–
1% Pt/Al_2O_3	565	93	–
$Ba(NO_3)_2/Al_2O_3$	542	85	34
1% Pt-$Ba(NO_3)_2/Al_2O_3$	514	91	39
$Sr(NO_3)_2/Al_2O_3$	509	86	36
1% Pt-$Sr(NO_3)_2/Al_2O_3$	484	97	140
$Ca(NO_3)_2/Al_2O_3$	486	81	133
1% Pt-$Ca(NO_3)_2/Al_2O_3$	470	92	127

catalyst was studied in Ref. [43] and it was found that optimal reaction rates are observed at temperatures around 350 °C, where equilibrium concentrations of NO_2 in its mixture with NO and oxygen are still quite high, up to 60%. Above this temperature, the effects of the equilibrium boundary are observed while below this temperature the conversion of soot is still kinetically limited as shown on Fig. 10. Therefore, in the case of Ba-based system, where NO_X are released at much higher temperatures, above 500–600 °C the effect of Pt addition is quite negligible, since at that temperature NO_X mainly consist of nitrogen monoxide. For Sr- and Ca-based systems NO_X release occurs within required temperature interval and as a consequence Pt helps to convert NO to NO_2 and overall soot oxidation efficiency is increased substantially (Table 4).

The effect of the Pt can be twofold: besides the additional recycling of NO to NO_2 Pt can also influence the temperature of the nitrates decomposition. For the Ba-based system it is known [27,36,44] that in the presence of Pt nitrates decompose at a lower temperature than in case of samples without Pt. It was already discussed before that the NO_X assisted soot oxidation probably has a volcano-shape dependency on the temperature when the rate of the soot oxidation is limited from one side by the equilibrium concentration of NO_2 and from the other side the kinetics of the soot oxidation. So the optimal interval is supposed to be between 350 and 450 °C, which coincide with temperature of the decomposition of $Ca(NO_3)_2$, and can account for extremely high efficiency of this system. In the Sr-based system the temperature of the maximum of the nitrates decomposition is ~550 °C, which is quite far from the optimal interval, but after the introduction of Pt the nitrates in the Sr-based system start decomposing at a much lower temperature, around 500 °C, which is more favourable for the soot oxidation. In the case of the Ca-based system which was already close to the optimum, the addition of Pt leads to a further decrease of the temperature for nitrates decomposition in the direction of the region where the reaction of the soot oxidation is still kinetically limited and, therefore, the addition of Pt in the Ca case does not seem to improve the catalytic performance much, only the selectivity to CO_2 becomes higher.

4. Conclusion

The stability of supported nitrates and temperature of NO_X release increase parallel to the basicity of the cation while available NO_X storage capacity decreases. Pre-treatment of the catalysts in reducing conditions at high temperatures leads to a significant increase in available NO_X storage capacity. The presence of soot favours the decomposition of surface nitrates and in the presence of stored nitrates soot is oxidized through two routes: oxidation with NO_2 and oxidation with O_2. Therefore, the stored nitrates contribute to the soot oxidation and help to lower the temperature of soot oxidation up to almost 100 °C. Most efficient soot oxidation is achieved in the case when there is a match between the temperature of nitrates decomposition and temperature of soot oxidation by NO_2. However, in the presence of only NO_X storage material in most cases the efficiency of NO_X utilization is quite low, around 30% due to low thermodynamic stability of NO_2 at high temperatures. Therefore, platinum as an oxidation catalyst is essential to increase the efficiency of NO_X utilization for soot oxidation up to 140% and selectivity to CO_2. A combination of oxidation catalyst with NO_X storage materials enables to lower the temperature of soot oxidation more than 100 °C.

Acknowledgements

Chemical company BASF is acknowledged for financial support. The X-Ray facilities of the Department of Materials Science and Engineering of the Delft University of Technology is acknowledged for the X-Ray analysis.

References

[1] http://www.dieselnet.com/standards/eu/.
[2] S. Matsumoto, Catal. Today 90 (2004) 183.
[3] J.P.A. Neeft, M. Makkee, J.A. Moulijn, Appl. Catal. B 8 (1996) 57.
[4] B.A.A.L. Setten, M. Makkee, J.A. Moulijn, Catal. Rev. Sci. Eng. 43 (2001) 489.
[5] J.P.A. Neeft, O.P. van Pruissen, M. Makkee, J.A. Moulijn, Appl. Catal. B12 (1997) 21.
[6] J.P.A. Neeft, M. Makkee, J.A. Moulijn, Fuel Proc. Tech. 47 (1996) 1.
[7] S.J. Jelles, J.P.A. Neeft, B.A.A.L. van Setten, M. Makkee, J.A. Moulijn, Stud. Surf. Sci. Catal. 116 (1998) 621.
[8] J.B. Howard, W.J. Kausch, Prog. Energy Combust. Sci. 6 (1980) 263.
[9] J.P.A. Neeft, M. Makkee, J.A. Moulijn, Chem. Eng. J. 64 (1996) 295.
[10] J.P.A. Neeft, M. Makkee, J.A. Moulijn, Fuel 77 (1998) 111.
[11] G. Mul, J.P.A. Neeft, F. Kapteijn, M. Makkee, J.A. Moulijn, Appl. Catal. B 30 (1995) 339.
[12] S.J. Jelles, B.A.A.L. van Setten, M. Makkee, J.A. Moulijn, Appl. Catal. B 21 (1999) 35.
[13] A. Setiabudi, N.K. Allaart, M. Makkee, J.A. Moulijn, Appl. Catal. B 60 (2005) 233.
[14] G. Mul, J.P.A. Neeft, M. Makkee, F. Kapteijn, J.A. Moulijn, Stud. Surf. Sci. Catal. 116 (1998) 645.
[15] J.P.A. Neeft, W. Schipper, G. Mul, M. Makkee, J.A. Moulijn, Appl. Catal. B 11 (1997) 365.
[16] A. Bueno-Lopez, K. Krishna, M. Makkee, J.A. Moulijn, J. Catal. 230 (2005) 237.
[17] I. Atribak, A. Bueno-Lopez, A. Garcia-Garcia, Catal. Commun. 9 (2008) 250.
[18] K. Krishna, A. Bueno-Lopez, M. Makkee, J.A. Moulijn, Appl. Catal. B 75 (2007) 189.
[19] J. Liu, Z. Zhao, C.M. Xu, A. Duan, Appl. Catal. B 78 (2008) 61.
[20] D. Fino, N. Russo, G. Saracco, V. Specchia, Powder Tech. 180 (2008) 74.
[21] B.J. Cooper, J.E. Thoss, SAE 890404, Detroit (1989).
[22] A. Setiabudi, M. Makkee, J.A. Moilijn, Appl. Catal. B 42 (2003) 35.
[23] A. Setiabudi, M. Makkee, J.A. Moulijn, Appl. Catal. B 50 (2004) 185.
[24] K. Krishna, M. Makkee, Catal. Today 114 (2006) 48.
[25] E. Jobson, Top. Catal. 28 (2004) 191.
[26] J. Suzuki, S. Matsumoto, Top. Catal. 28 (2004) 171.
[27] L.J. Gill, P.G. Blakeman, M.V. Twigg, A.P. Walker, Top. Catal. 28 (2004) 157.
[28] M. Takeuchim, S. Matsumoto, Top. Catal. 28 (2004) 151.
[29] G. Zhou, T. Luo, R.J. Gorte, Appl. Catal. B 64 (2006) 88.
[30] V.G. Milt, C.A. Querini, E.E. Miró, M.A. Ulla, J. Catal. 220 (2003) 424.
[31] T. Szailer, J.H. Kwak, D.H. Kim, J. Szanyi, C. Wang, C.H.F. Peden, Catal. Today 114 (2006) 86.
[32] A. Amberntsson, H. Persson, P. Engström, B. Kasemo, Appl. Catal. B 31 (2001) 27.
[33] H. Mahzoul, J.F. Brilhac, P. Gilot, Appl. Catal. B 20 (1999) 47.
[34] F. Laurent, C.J. Pope, H. Mahzoul, L. Delfosse, P. Gilot, Chem. Eng. Sci. 58 (2003) 1793.
[35] P. Broqvist, H. Grönbeck, E. Fridell, I. Panas, Catal. Today 96 (2004) 71.
[36] D. James, E. Flourre, M. Ishii, M. Bowker, Appl. Catal. B 45 (2003) 147.
[37] Ch. Sedlmair, K. Seshan, A. Jentys, J.A. Lercher, J. Catal. 214 (2003) 308.
[38] I. Atribak, I. Such-Basáñez, A. Bueno-López, A. Garcia-Garcia, J. Catal. 250 (2007) 75.
[39] V. Milt, M.L. Pisarello, E.E. Miró, C.A. Querini, Appl. Catal. B 41 (2003) 397.
[40] S.-J. Huang, A.B. Walters, M.A. Vannice, Appl. Catal. B 17 (1998) 183.
[41] Inorganic Crystal Structure Database, http://icsdweb.fiz-karlsruhe.de.
[42] American Mineralogist Crystal Structure Database, http://rruff.geo.arizona.edu/AMS/.
[43] W.S. Epling, L.E. Campbell, A. Yezerets, N.W. Currier, J.E. Parks, Catal. Rev. 46 (2004) 163.
[44] F. Prinetto, G. Ghiotti, I. Nova, L. Lietti, E. Tronconi, P. Forzatti, J. Phys. Chem. B 105 (2001) 12732.
[45] S.-J. Huang, A.B. Walters, M.A. Vannice, J. Catal. 192 (2000) 29.
[46] V. Medhekar, V. Balakotaiah, M.P. Harold, Catal. Today 121 (2007) 226.
[47] Reaction Web Database, http://www.crct.polymtl.ca/reacweb.htm.